J. Phys. Chem. A **2009,** *113,* 14029–14038

Hydrates of Copper Dichloride in Aqueous Solution: A Density Functional Theory and Polarized Continuum Model Investigation

Fei-Fei Xia,[†] Hai-Bo Yi,*,[†] and Dewen Zeng*,[‡]

College of Chemistry and Chemical Engineering, Hunan University, Changsha, Hunan 410082, China, and College of Chemistry and Chemical Engineering, Central South University, Changsha, Hunan 410083, China

Received: April 21, 2009; Revised Manuscript Received: October 25, 2009

In this work, the hydrates of copper dichloride in gas and aqueous phase have been investigated using the B3LYP method. Low-lying conformers of $CuCl_2(H_2O)_n$ clusters for $n = 1-10$ were obtained by an extensive conformation search. Contact ion pair (CIP) and solvent-shared ion pair (SSIP) with one dissociated chloride atom (SSIP/s) and SSIP with two dissociated chloride atoms (SSIP/d) all were considered. Our calculations present such a trend that a four-fold CIP conformer is more favorable for $CuCl_2(H_2O)_n$ cluster ($n \leq 7$) and four-fold SSIP/s for $n = 8-10$ in the gas phase, while in aqueous solution, more stable structures are five-fold SSIP/s conformer for $n = 7-9$ and four-fold CIP conformer for $n = 2-6$. Hydrogen bond (HB) plays an important role in the $CuCl_2$ solvation, especially HBs formed between the first and second solvation shell water molecules. Electronic absorption spectra of $CuCl_2(H_2O)_n$ clusters were obtained using long-range-corrected time-dependent density functional theory. The calculated electronic absorption peak around 270 nm of CIP conformers is coincident with the absorption of $[CuCl_2]^0_{aq}$ species resolved from the spectra obtained in solutions of trace $CuCl_2$ (ca. 10^{-5} mol/kg) + LiCl (0−18 m), while those of SSIP/s (∼250 nm) and SSIP/d (∼180 nm) conformers probably correspond to the absorption spectra of $[CuCl]^+_{aq}$ and $[Cu]^{2+}_{aq}$ species, respectively. Natural bond orbital charge population analyses show that charge transfer (CT) between a central copper(II) atom and ligands (Cl and H_2O) increases as the hydrated cluster expands, especially CT from Cu^{2+} to the first solvation shell, which enhances the strength of HBs. Such CT becomes more apparent for SSIP structure with the dissociation of chloride ion. OH stretching vibration frequencies of proton donor type water in $CuCl_2(H_2O)_n$ clusters are obviously red-shifted in comparison to those of water clusters, due to CT between the central atom Cu and ligands. SSIP conformers have apparent IR absorption peaks of OH stretching vibration at ∼3000 cm^{-1} for the effect of half-dissociated chloride atoms.

1. Introduction

Copper dichloride solution is usually involved in chemical engineering processes, especially in a chloride hydrometallurgical process.[1−3] As with many other heavy metal ions, the Cu^{2+} ion possesses the potential to form complexes with Cl^- ion in aqueous solution, which gives the $CuCl_2$ solution special properties when it is mixed with Cl^--donating salt.[4−6] To understand the formation process of a $CuCl_n$ complex, including the formation constant of the complexes in each step, scientists investigated the copper(II) chloride aqueous solution with the help of UV−vis spectra,[7−11] assuming that complexes in the statistic ratios as $[Cu]^{2+}_{aq}$, $[CuCl]^+_{aq}$, $[CuCl_2]^0_{aq}$, $[CuCl_3]^-_{aq}$, and $[CuCl_4]^{2-}_{aq}$ species are present in the solution. By resolution of experimental UV−vis spectra, they obtained the concentration distribution of the above various species in a specific condition, as well as the absorption spectrum of each species assigned. Herein, an interesting question is whether the resolved absorption spectrum corresponds to the species assigned. Exactly how are the structures of the species assumed? As it is well-known, the Cu^{2+} ion tends to coordinate with the water molecule besides the Cl^- ion. The coordination competition of the water molecule and Cl^- ion must lead to different conformers for a same statistic species when their environmental conditions change. For example, the statistic aqueous $CuCl_2$ complex may be contact ion pair (CIP) formed between Cu^{2+} and Cl^- or solvent-shared ion pair (SSIP). The answer to these questions will enable us to understand the structure of the hydrated cupric chloride complex more exactly, as well as the influence of water activity on the association constant of the complex $[CuCl_n]^{2-n}_{aq}$ and the interaction of $CuCl_2$ with Cl^--donating salt in aqueous solution. Therefore, we intend to carry out a series of quantum calculations on $CuCl_m(H_2O)_n$ hydrates in aqueous solution.

One way of approaching the structure and properties of the aqueous solution of salts involves using a quantum chemical method to examine clusters of a salt formed by water molecules. Recently, the salt of alkali metal ions and halide anions was intensively investigated using ab initio method and density functional theory (DFT).[12−17] The theoretical calculations by Kim et al.[14−16] showed the presence of the CIP and SSIP conformers for the salt of alkali metal ions and halide anions in solution and provided a lot of information for experiment with the dissociation phenomenon. Their work showed the possibility using a quantum chemical method to investigate the structure and properties of electrolytes in solution.

So far, copper−water complexes have been studied intensively with respect to their lowest conformations and the coordination number in the gas and aqueous phases both theoretically[18−23] and experimentally.[24−28] It is reported that[18,22,29,30] Cu^{2+} complexes prefer four- or five-coordination, which is different than Cu^+ complexes, in some cases six-coordination.

---

* To whom correspondence should be addressed. E-mail: hbyi@hnu.cn and dewen_zeng@hotmail.com.

[†] Hunan University.

[‡] Central South University.

10.1021/jp909092p

However, copper(II) chloride water complexes were not focused on as copper(II)−water complexes. Recently, Shang et al.[31] have investigated the transportation of $CuCl_2$ as hydrated species $CuCl_2(H_2O)_n^{gas}$ in water vapor with statistical hydration numbers of 4.0, 3.6, and 3.3 at 330, 350, and 370 °C, respectively, but is still unclear which species of the hydrated copper dichloride existed in the gas phase. In order to gain an insight into these problems, a theoretical investigation of copper(II) chloride complexation both in the gas and aqueous phases is very desirable. However, due to the complication of Cu^{2+} hydrates with the approaching of Cl^-, as the first step, we focused our theoretical investigation on the relatively simple copper dichloride hydrates both in the gas and aqueous phases.

Salt dissociation involves a cooperative process between salt and water molecules. As water molecules are successively incorporated, the cation−anion distance in the salt increases gradually, resulting in an ion pair separated structure. Therefore, in this investigation, the relative stability of dissociated and undissociated forms for $CuCl_2(H_2O)_n$ ($n = 1-10$) clusters in the gas and aqueous phases was investigated using DFT, as well as the role of hydrogen bonds (HBs). Furthermore, the electronic absorption spectra of some typical $CuCl_2(H_2O)_n$ clusters were calculated using long-range-corrected time-dependent density functional theory (LRC-TDDFT)[32−34] in this paper. Our theoretical spectra were compared with the experimental absorption peaks of $[CuCl_2]^0_{aq}$ species resolved from the spectra obtained in the solutions of trace $CuCl_2$ (ca. 10^{-5} mol/kg) and LiCl (0−18 mol/kg),[10] and the structures of experimental resolved species were also assigned. Therefore, a theoretical study of electronic absorption spectra, combined with theoretical investigation of cluster structures for $CuCl_2(H_2O)_n$ complexes, is included in this work. Infrared spectra (IR) are very useful to investigate the structure of hydrated clusters, especially for their OH stretching vibration. Insight into the structure of such species can be gained from vibrational frequency analysis, as the IR spectra along with ab initio calculation provide the fingerprints of various molecular clusters.[35−38] So IR spectra for water clusters and $CuCl_2(H_2O)_n$ clusters are also included in the following section. In addition, natural bond orbital (NBO) charge population analyses for $CuCl_2(H_2O)_n$ complexes were carried out to understand the role of HBs in CIP and SSIP conformers.

2. Calculations and Methods

The works of Kim et al. investigated the hydration of NaX, KX (X = F, Cl, Br, I) and CsF using DFT with Becke's three-parameter exchange potential and Lee−Yang−Parr correlation functional (B3LYP), Møller−Plesset second-order perturbation theory (MP2), and coupled cluster theory with single, double, and perturbative triple excitations (CCSD(T)), but the results obtained using these methods lead to a similar conclusion on the structure and dissociation behaviors.[14−16] Meanwhile, the works of Sodupe and Rodriguez-Santiago et al.[39,40] also showed that the hybrid DFT methods, in particular, the B3LYP one, provide very similar structural parameters for systems with similar spin density distribution, and that the B3LYP relative energies are in good agreement with those determined by highly correlated electronic structure methods, such as MP2 and CCSD(T). Therefore, B3LYP method was chosen to look for local minimum energy structures of $CuCl_2(H_2O)_n$ ($n = 1-10$) clusters. On generating initial hydrated structures, various coordination and HBs are considered, followed by geometry optimization to obtain a local minimum energy structure. Dunning's correlation consistent basis sets[41] were employed, that is, aug-cc-pVDZ for the nonmetallic elements O, H, and Cl. For Cu, the relativistic effective core potentials (RECP) developed by the Stuttgart group were used in conjunction with the basis set to describe the metal valence electrons, and a set of two f and one g polarization functions was added.[42] The valence space was described by the corresponding (6s5p3d) basis sets. This basis set combination is abbreviated as aVDZ. The basis set superposition error[43] (BSSE) correction was taken into account. It is well-known that TDDFT becomes widely used as a simple method for rapid and accurate calculations of molecular excitation energies. It has, however, been reported that conventional TDDFT calculations underestimate Rydberg excitation energies, oscillator strengths, and charge-transfer excitation energies. Tawada et al.[32] supposed that this problem may also come from the lack of long-range exchange interaction and applied the LRC scheme to TDDFT calculations. Therefore, electronic excited state calculations of typical copper dichloride hydrates at LRC-TDDFT/aVDZ level were carried out using Q-Chem software package.[32−34,44] In addition, the NBO calculations[45−47] and frequency analysis for $CuCl_2(H_2O)_n$ conformers were also performed at the B3LYP/aVDZ level. Recently, Goddard et al.[48] and Clark et al.[49] employed mixed cluster/continuum models to investigate the solvation of Cu^{2+} and Pb^+, respetively, and their calculated results all agree well with experimental observations. Thus, to consider the long-range electrostatic solvent effect, we employed single-point polarized continuum model (PCM)[49−51] in the calculation of hydration energy for various aqueous hydrated $CuCl_2$ clusters. All geometry optimization, frequency, and NBO calculations were carried out with Gaussian 03 software package.[52]

Stabilities of different $CuCl_2(H_2O)_n$ complexes for $n = 1-10$ can be compared using hydration energies(ΔE):

$$\Delta E = E_{CuCl_2(H_2O)_n} - E_{CuCl_2} - E_{(H_2O)_n} \qquad (1)$$

which corresponds to the process

$$CuCl_2 + (H_2O)_n \rightarrow CuCl_2(H_2O)_n$$

Thermodynamics values for G_{solv} were obtained using PCM within the context of

$$\Delta G_{solv} = G_{CuCl_2(H_2O)_n} - G_{CuCl_2} - G_{(H_2O)_n} \qquad (2)$$

The free energy of a species is expressed as

$$G_{solv} = E^0_{gas} + G_{corr} + G_{scrf} + G_{ss} \qquad (3)$$

where $G_{corr} = PV - TS$, and E^0_{gas} is the hydration energy of standard state (298.15 K, 1 atm) in the gas phase, and

$$G_{scrf} = G_{electrostatic} + G_{nonelectrostatic} = G_{electrostatic} + G_{cavition} + G_{dispersion} + G_{repulsion} \qquad (4)$$

In the case of water

$$G_{ss} = RT\ln(P_w/P^0)/n \qquad (5)$$

P_w is the pressure of liquid water assuming it is an idea gas, P^0 is the pressure of the gas phase standard state, R is the universal gas constant, and T is the room temperature in kelvin.

In the hydration process of $CuCl_2$, one may consider there is an approximate boundary between the inner solvation shell, which should be considered using a quantum mechanics methods, and outer solvation shell mainly having a long electrostatic effect on ions which can be considered as continuum medium. An approximation to a complete solvation shell around copper dichloride is that the binding energy of the mth water molecule in $CuCl_2(H_2O)_m$ clusters is close to the estimated dissociation energy of one water molecule from liquid water or

SCHEME 1: Approximation for Complete Solvation Shell of Ions or Ion Pairs

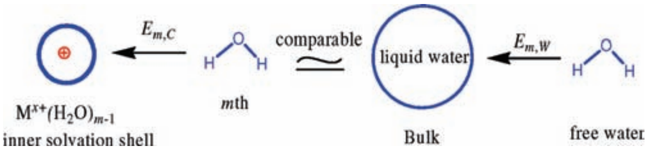

water clusters in absolute value (Scheme 1). Since the hydration energy of each water molecule does not change linearly as the hydrated cluster expands, a more appropriate approximation of the complete solvation shell of ions or ion pairs is on the condition that the binding energies of the (m+1)th and (m+2)th water molecules are also close to the dissociation energy of one water molecule from liquid water in absolute value.

The binding energy for the additive water molecule in $CuCl_2(H_2O)_m$ cluster is defined as

$$\Delta E_{m,\mathrm{C}} = E_{\mathrm{CuCl_2(H_2O)}_m} - E_{\mathrm{CuCl_2(H_2O)}_{m-1}} - E_{\mathrm{H_2O}} \qquad (6)$$

The dissociation energy $\Delta E_{m,\mathrm{W}}$ of one water molecule from bulk liquid water is ~10.5 kcal/mol estimated from the evaporate energy of liquid water.[48,53]

3. Results and Discussion

We have investigated various different conformers of hydrated $CuCl_2$ clusters using B3LYP/aVDZ methods. Both CIP and SSIP conformers were considered in optimization of $CuCl_2(H_2O)_n$ clusters. For SSIP conformers, SSIP/s (one Cl atom separated by solvation shell water molecules) and SSIP/d (two Cl atoms separated by solvation shell water molecules) conformations were both considered. In addition, HBs were taken into account for hydrated $CuCl_2$ clusters, especially HB formed between the first and second solvation shells (called α-HB), HB formed between the second and third solvation shells (called β-HB), HB formed between the third and fourth solvation shells (called γ-HBs), and ionic HB formed between chloride atom and water molecules (called IHB). For the formation of HBs in $CuCl_2(H_2O)_n$, we have considered that a water molecule acts as proton donor or acceptor in the formation of single or double HBs and HB network.

3.1. Structures and Energetics. We have carried out extensive calculations for searching the low-lying conformers of the $CuCl_2(H_2O)_n$ ($n = 1-10$) cluster in the gas phase at the B3LYP/aVDZ level, intending to determine the most stable structure of each $CuCl_2(H_2O)_n$ ($n = 1-10$) cluster at a certain metal coordination number (4−6). As a consequence, the hydration energy change of each $CuCl_2(H_2O)_n$ ($n = 1-10$) as a function of metal coordination number (4−6) has been determined. Typical optimized geometries and NBO charge population results of $CuCl_2(H_2O)_n$ ($n = 1-10$) clusters are presented in Figure 1, where the six-fold SSIP conformers (SSIP/s and SSIP/d) were excluded because they are far more unstable according to our calculation. The works of Morokuma et al. indicated that NBO calculation may probably leave the p orbitals in the Rydberg space, and those orbitals can contribute significantly to the overall charge,[54,55] and our NBO charge population analyses just showed that the p orbitals are obviously involved in charge transfer or coordination bonding for the orbital configuration of Cu^{2+} in W7-A ($3d^{9.33}4s^{0.37}4p^{0.41}$) and W7-C ($3d^{9.27}4s^{0.33}4p^{0.48}$) conformers. Table 1 lists different energy parameters for $CuCl_2(H_2O)_n$ ($n = 1-10$) clusters using the B3LYP/aVDZ method. The bond lengths of some typical conformers are presented in Table 2.

The Cu−Cl bond length of monohydrated copper dichloride cluster increases by 6.4 pm, compared to that of $CuCl_2$ molecule, and its calculated complex hydration energy is −14.0 kcal/mol. As n increases to 2, a regular square-planar geometry (W2-A) was obtained; the Cu−Cl bond length further lengthens by 8.2 pm, and its hydration energy increases to −25.1 kcal/mol. For $CuCl_2(H_2O)_3$, W3-A is the most stable four-fold conformer in hydration energy, whose structure has an α-HB and an IHB, and the bond length of α-HB in W3-A (166.5 pm) is 27.8 pm shorter than that of HB in the dimer water cluster (194.3 pm). Meanwhile, the formation of these HBs also makes the Cu−Cl bond lengthen nearly 3.6 pm and the Cu−O bond shorten about 4.3 pm.

In the case of tetrahydrated $CuCl_2(H_2O)_4$ cluster, four-fold CIP conformer (W4-A) that has two α-HBs and IHBs is also the most stable structure in hydration energy. Due to the formation of such HBs, the Cu−O bond length becomes shorter, and the Cu−Cl bond length becomes longer. However, W4-B with an α-HB, an IHB, and a β-HB is less stable than W4-A in the gas phase. Similarly, for $CuCl_2(H_2O)_n$ clusters ($n = 5$ and 6), the Cu−O bond length is shortened and the Cu−Cl bond length is lengthened. Four-fold CIP conformer is also the most stable structure for the heptahydrated cluster, but this conformer is a four-fold reticular CIP structure, whose solvation shell water molecules form rings (HB network), and its calculated hydration energy is −33.7 kcal/mol. We found that the four-fold CIP conformer is also the most stable structure for $CuCl_2(H_2O)_n$ clusters ($n = 2-7$) of all the optimized conformers (as shown in Figure 1), and the average Cu−O and Cu−Cl distances of these four-fold CIP conformers are 195.9−202.5 and 222.5−226.6 pm, respectively. Meanwhile, in concentrated aqueous copper dichloride solutions, the average Cu−O and Cu−Cl distances are 195−196 and 225−229 pm by X-ray diffraction technique,[56,57] 196(3) and 230−350 pm from neutron diffraction experiments of $CuCl_2$ salt in a 4 M aqueous solution.[58] Therefore, it can be noted that the bond lengths of CIP conformers obtained in our calculations generally agree with the experimental observations (4 mol/kg aqueous solution).[58] Since the binding energies of the fifth, sixth, and seventh water molecules are already close to the calculated dissociation energy of one water molecule in the liquid phase in absolute value, it can be concluded that the hydrated $CuCl_2(H_2O)_n$ cluster approaches the complete solvation shell as n increases to 5−7 (as shown in Figure 2).

In the case of the octahydrated cluster, four-fold SSIP/s conformer (W8-D) becomes 0.7 kcal/mol more stable than the CIP conformer, W8-A. Compared with W8-A, the Cu−O bond length of W8-D is further shortened and one Cu−Cl bond length increases to 409.5 pm. Meanwhile, the average Cl−H bond length of W8-D is apparently shorter than that of W8-A, which indicates that the dissociation of Cl^- accompanying the enhancement of IHBs. NBO charge population analyses show that the charges on copper (1.03e) and chloride atoms (−0.77 and −0.58e) of W8-D are obviously larger than those of W8-A (Cu/0.89e, Cl/−0.59e,−0.62e), which suggests that the chloride atom tends to dissociate as n increases to 8. Therefore, for CIP $CuCl_2(H_2O)_n$ clusters, seven water molecules may be the upper limitation in inner solvation shell because a four-fold SSIP/s conformer becomes a more stable structure when the eighth water molecule is involved. The four-fold SSIP/s conformer, W9-D, is iso-energetic with W9-A. It is to be noted that one chloride atom tends to dissociate (Cu−Cl bond length as shown in Table 2). The charge of the dissociated Cl atom in the W9-D structure is −0.78e, which also implies that the chloride atom tends to dissociate (Figure 1).

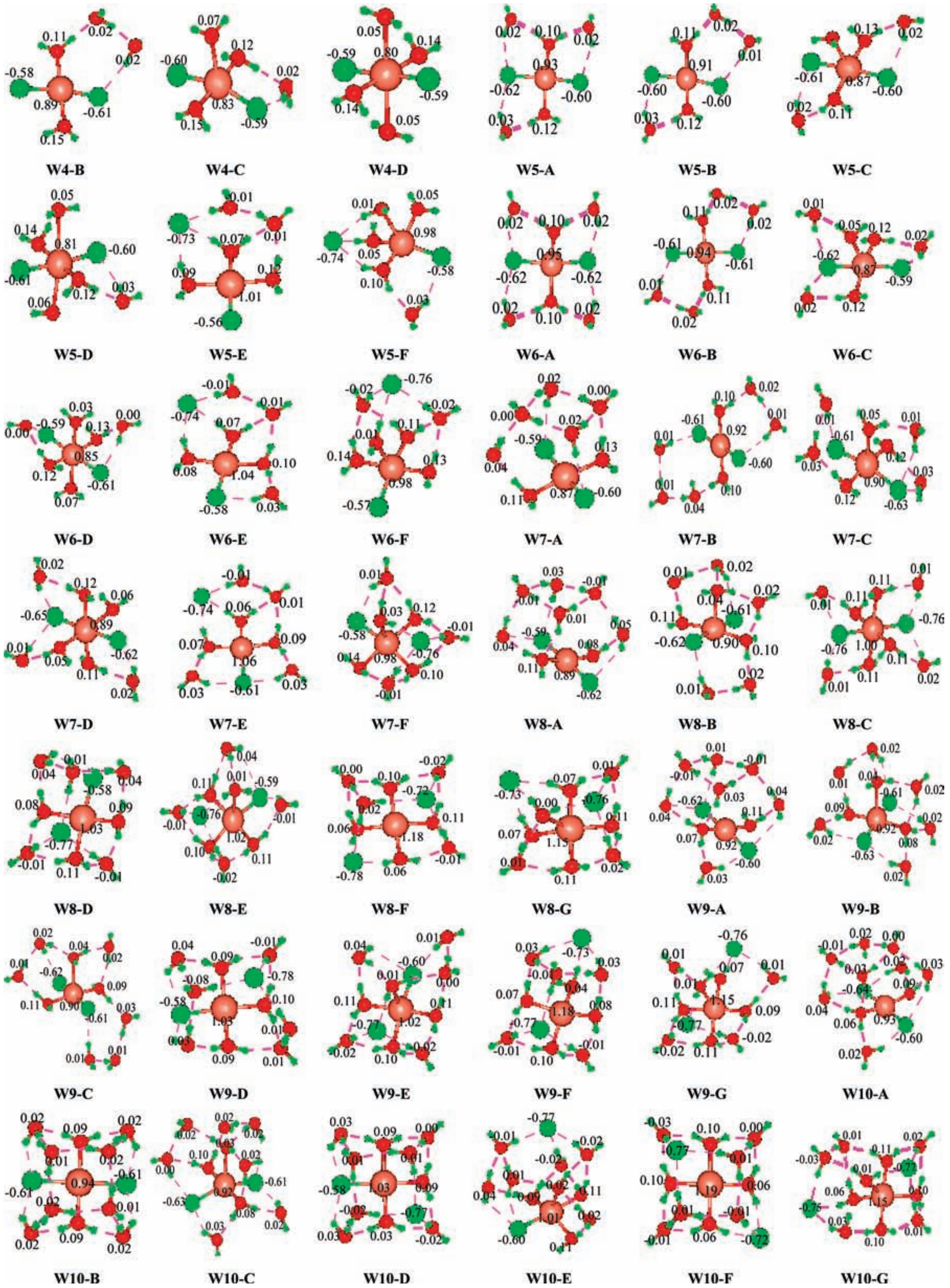

Figure 1. Typical optimized structures of $CuCl_2(H_2O)_n$ for $n = 1-10$ at the B3LYP/aVDZ level, and NBO charge population analyses for copper atom, chloride atom, and water molecules are also presented. Other optimized structures that are quite less stable both in the gas and aqueous phases were not collected. W is the abbreviation of water. The hydrogen bonds formed among water molecules are shown by the bold dashed line, and those formed between water molecules and chloride atom by a thin dashed line. NBO charge is given in au/*e*.

When *n* increases to 10, four-fold SSIP/s conformers (W10-D) are of 3.5 kcal/mol more stable than the four-fold CIP conformer (W10-A). The Cu−O bond length is further shortened, and Cu−Cl bond length is further lengthened (as shown in Table 2). Meanwhile, four-fold SSIP/d conformer (W10−F) is only 3.9 and 0.4 kcal/mol less stable than its SSIP/s (W10-D) and CIP (W10-A) structures in the gas phase. For the SSIP/d conformer (W10-F), its two Cu−Cl bond lengths increase to 387.2 and 452.6 pm, which indicates that the second chloride atom also tends to dissociate. NBO charge population analyses gain the same conclusion, as shown in Figure 1.

TABLE 1: B3LYP/aVDZ Hydration Energies of $CuCl_2(H_2O)_n$ Clusters for $n = 1-10$ in the Gas and Aqueous Phases[a]

geometries		*CN*	gas phase				aqueous phase[b]		
			ΔE	ΔE_0	ΔH	ΔG	ΔE_{solv}	$\Delta E_{solv,0}$	ΔG_{solv}
CIP	**W1**	**3**	**−14.0**	**−1.7**	**−2.5**	**6.0**			
CIP	**W2-A**	**4**	**−25.1**	**−22.4**	**−23.5**	**−11.1**			
CIP	**W3-A**	**4**	**−27.7**	**−25.9**	**−26.5**	**−14.8**			
	W3-B	5	−21.4	−20.2	−20.2	−9.6			
CIP	**W4-A**	**4**	**−27.2**	**−25.8**	**−26.2**	**−14.6**	**−29.0**	**−27.6**	**−16.4**
	W4-B	4	−24.3	−23.1	−23.4	−12.9	−28.2	−27.0	−16.8
	W4-C	5	−21.3	−20.6	−20.4	−9.8	−26.5	−25.8	−15.0
	W4-D	6	−14. 6	−14.9	−13.8	−6.1	−20.7	−21.0	−12.2
CIP	**W5-A**	**4**	**−27.9**	**−26.6**	**−26.9**	**−14.6**	−28.1	−26.8	−14.8
	W5-B	4	−27.4	−25.9	−26.4	−14.5	**−28.6**	**−27.1**	**−15.7**
	W5-C	5	−24.1	−23.1	−23.2	−11.6	−26.8	−25.9	−14.3
	W5-D	6	−17.3	−17.4	−17.1	−6.0	−21.6	−21.7	−10.3
SSIP/s	W5-E	4	−23.4	−21.2	−22.5	−7.6	−25.4	−23.2	−9.7
	W5-F	5	−16.6	−15.3	−16.1	−2.2	−21.6	−20.3	−7.3
CIP	**W6-A**	**4**	**−29.9**	**−28.3**	**−28.7**	**−15.7**	−28.9	−27.4	−14.8
	W6-B	**4**	−29.3	−27.4	−28.2	−15.8	**−29.6**	**−27.7**	**−16.1**
	W6-C	5	−26.6	−24.9	−25.5	−11.1	−27.7	−26.0	−12.2
	W6-D	6	−20.9	−19.7	−19.8	−6.4	−22.3	−21.2	−7.9
SSIP/s	W6-E	4	−27.5	−24.8	−26.5	−9.7	−27.9	−25.2	−10.1
	W6-F	5	−25.4	−22.5	−24.2	−6.5	−28.3	−25.4	−9.4
CIP	**W7-A**	**4**	**−33.7**	**−31.3**	**−32.4**	**−17.6**	−30.7	−28.3	−14.7
	W7-B	**4**	−29.8	−29.5	−29.4	−20.8	**−31.8**	**−31.6**	**−22.9**
	W7-C	5	−28.4	−27.8	−27.8	−16.0	−30.7	−30.7	−18.3
	W7-D	6	−21.9	−22.5	−21.7	−12.2	−26.2	−26.9	−16.5
SSIP/s	W7-E	4	−28.1	−27.2	−27.9	−15.4	−30.8	−29.9	−18.1
	W7-F	**5**	−28.3	−24.8	−26.5	−9.7	**−31.9**	**−29.8**	**−17.9**
CIP	**W8-A**	**4**	**−24.2**	**−23.5**	**−23.6**	**−12.5**	−25.1	−24.3	−13.3
	W8-B	**5**	−20.3	−21.0	−20.2	−12.1	**−25.8**	**−26.6**	**−17.6**
	W8-C	6	−13.8	−14.8	−14.2	−4.9	−23.0	−23.9	−14.0
SSIP/s	**W8-D**	**4**	**−24.9**	**−23.8**	**−24.3**	**−11.4**	−26.3	−25.1	−12.8
	W8-E	**5**	−23.0	−22.0	−22.4	−10.0	**−27.1**	**−26.2**	**−14.1**
SSIP/d	W8-F	4	−17.8	−16.6	−18.1	−3.4	−23.1	−21.9	−8.7
	W8-G	5	−17.8	−16.4	−17.8	−2.69	−24.8	−23.4	−9.6
CIP	**W9-A**	**4**	**−26.2**	**−25.5**	**−25.5**	**−14.2**	−24.4	−23.7	−12.4
	W9-B	5	−20.4	−21.2	−22.8	−10.7	−24.3	−25.2	−14.6
	W9-C	5	−20.0	−20.9	−20.7	−12.5	−24.9	−25.8	−17.4
SSIP/s	**W9-D**	**4**	**−25.5**	**−24.4**	**−25.0**	**−12.3**	−26.7	−25.6	−13.4
	W9-E	**5**	−23.5	−22.4	−22.8	−9.9	**−27.2**	**−26.1**	**−13.6**
SSIP/d	W9-F	4	−17.0	−16.7	−18.3	−2.7	−21.0	−20.3	−6.3
	W9-G	5	−16.7	−15.6	−16.8	−1.9	−23.5	−22.4	−8.6
CIP	**W10-A**	**4**	**−28.7**	**−28.3**	**−28.1**	**−17.4**	−24.6	−24.2	−13.3
	W10-B	4	−25.0	−23.7	−23.7	−11.7	−27.4	−26.1	−14.2
	W10-C	5	−25.1	−25.4	−24.7	−15.6	−26.8	−27.2	−17.4
SSIP/s	**W10-D**	**4**	**−32.2**	**−30.2**	**−31.5**	**−16.5**	**−30.4**	**−28.4**	**−14.7**
	W10-E	5	−28.2	−27.0	−27.7	−14.4	−27.6	−26.4	−13.8
SSIP/d	**W10-F**	**4**	**−28.3**	**−26.4**	**−22.7**	**−11.8**	**−29.0**	**−27.2**	**−12.5**
	W10-G	5	−24.1	−22.8	−24.2	−8.8	−27.5	−26.1	−12.2

[a] ΔE is hydration energy, ΔE_0 is zero-point-corrected electronic energies, ΔH and ΔG are enthalpies and free energies in the gas phase, ΔE_{solv} and ΔG_{solv} are hydration energies and free energies in the aqueous phase. CN is coordination number. All of the energies are in kcal/mol at room temperature (298 K and 1 atm). [b] Hydration energies, zero-point-corrected electronic energies, and free energies in the aqueous phase were obtained using the PCM-B3LYP/aVDZ method. Calculations of small $CuCl_2(H_2O)_n$ clusters ($n < 4$) using PCM-B3LYP/aVDZ are not suitable for investigating the hydration of $CuCl_2$ in the aqueous phase, and thus ΔE_{solv}, $\Delta E_{solv,0}$, and ΔG_{solv} of these clusters are not included in Table 1.

The theoretical calculations of Sukrat et al.[21] and experimental results of Pasquarello et al.[26] showed that copper(II)−water complexes prefer higher coordination number (five-fold). Our calculations of $CuCl_2(H_2O)_n$ clusters ($n = 2-10$) in the gas phase suggest that Cu^{2+} favors four-fold structure for its CIP and SSIP/s conformers, while its four- and five-fold conformers are almost energetically degenerate for the SSIP/d structure. However, as long-range electrostatic solvent effect is taken into account, five-fold conformers become more stable than its four-fold conformers, especially for SSIP/s conformation of $CuCl_2(H_2O)_n$ clusters ($n = 7-9$) in the aqueous phase. The SSIP/d conformer, W10-F, in the aqueous phase is only 1.4 kcal/mol less stable than the SSIP/s conformer W10-D and 1.6 kcal/mol more stable than the CIP conformer, W10-B, which indicates that the second chloride atom of $CuCl_2(H_2O)_{10}$ also tends to dissociate.

For $CuCl_2(H_2O)_n$ ($n = 4-8$) clusters, the d orbital energy splitting of the four-fold conformer is larger than that of five- and six-fold conformers, which indicates that the four-fold conformer would be more favorable in energy. Generally, as the hydration of $CuCl_2$ proceeds, the CT between Cu^{2+} and water molecules leads to copper(II) preferring higher coordination number (five-fold). As with the dissociation of Cl^-, the energy splitting of d orbitals for the five-fold SSIP conformer approaches or is larger than that of d orbitals for the four-fold SSIP conformer, and that of the five-fold SSIP/d conformer of

TABLE 2: Bond Lengths (in pm) of Some Selected $CuCl_2(H_2O)_n$ Clusters for $n = 0-10$[a]

geometries		R_{Cu-Cl1}	R_{Cu-Cl2}	R_{Cu-Cl}	R_{Cu-O1}	R_{Cu-O2}	R_{Cu-O}	$R_{\alpha HB}$	$R_{\beta HB}$	$R_{\gamma HB}$	R_{Cl-H}
$CuCl_2$		207.9	207.9	207.9							
W1	CIP	214.2	214.4	214.3	201.1		201.1				
W2	CIP	222.5	222.4	222.5	202.5	202.5	202.5				
W3-A	CIP	226.0	223.8	224.9	198.2	203.1	200.7	166.5			227.4
W4-A	CIP	227.3	227.3	227.3	198.5	198.6	198.6	167.5			226.4
W4-B	CIP	226.2	224.4	225.3	197.1	203.4	200.2	162.0	171.4		222.6
W5-A	CIP	230.1	228.0	229.1	195.4	199.3	197.4	171.3			228.9
W5-B	CIP	227.9	227.7	227.8	197.6	198.8	198.2	165.5			224.5
W6-A	CIP	230.8	230.7	230.7	196.0	195.9	195.9	173.0			228.9
W6-B	CIP	228.5	228.5	228.5	197.5	197.5	197.5	163.1	171.9		222.3
W7-A	CIP	228.8	226.6	227.7	198.1	201.0	199.6	167.8	182.4	182.3	244.4
W7-B	CIP	233.0	229.2	231.1	195.6	195.9	195.8	173.0	202.7		235.8
W7-D	SSIP/s	227.1	386.6	306.5	198.8	198.0	195.0	179.0	165.6		216.1
W8-A	CIP	228.9	225.0	227.0	198.8	200.5	199.7	180.7	185.7	181.2	249.9
W8-B	CIP	232.0	231.9	232.0	195.0	195.0	195.0	172.0	199.7		265.5
W8-D	SSIP/s	224.5	409.5	317.0	198.2	198.3	201.4	176.1	190.1		227.6
W9-A	CIP	229.8	228.1	229.0	197.5	199.1	198.3	177.9	185.6	181.2	247.7
W9-B	CIP	231.9	231.9	232.0	193.7	195.2	194.5	170.4	192.5	195.1	237.8
W9-D	SSIP/s	224.4	433.9	329.1	197.8	198.3	200.4	174.6	180.7		226.3
W10-A	CIP	232.2	229.3	230.7	196.2	198.0	197.1	178.5	186.6	180.8	244.7
W10-B	CIP	232.1	232.0	232.1	193.8	193.8	193.8	168.6	185.0	195.5	231.7
W10-D	SSIP/s	225.5	476.0	350.8	196.9	197.2	200.7	172.7	178.8	187.9	223.3
W10-F	SSIP/d	452.6	387.2	419.9	195.2	198.6	195.3	172.4	155.2	188.4	205.5

[a] R_{Cu-Cl} and R_{Cu-O} are the average Cu−Cl and Cu−O bond lengths, respectively, and R_{Cl-H} is the average Cl−H bond length. In concentrated aqueous copper dichloride solutions, the average Cu−O and Cu−Cl distances are 195−196 and 225−229 pm by X-ray diffraction technique,[56,57] 196(3) and 230−350 pm from neutron diffraction experiments of $CuCl_2$ salt in a 4 mol/kg aqueous solution.[58]

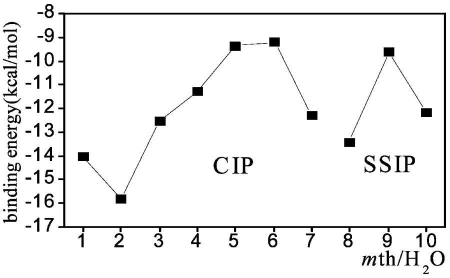

Figure 2. Binding energy of each water molecule calculated using eq 6 in the Calculations and Methods section. CIP and SSIP are the abbreviations of contact ion pair and solvent-shared ion pair, respectively. The dissociation energy of one water molecule from aqueous water estimated from its evaporate energy and sublimation energy is ∼10.5 kcal/mol.[48,53]

$CuCl_2(H_2O)_8$ is obviously larger than its four-fold conformer, as shown in Figure 3. From the view of ligand field, four-fold coordination is more favorable for a copper(II) atom with a coordination of two Cl^- and less water molecules ($n < 7$) involved in hydration of $CuCl_2(H_2O)_n$ clusters, while five-fold coordination is more favorable for a copper(II) atom when Cl^- tends to dissociate and more water molecules ($n > 7$) are involved in hydration.

In the dissolution process of $CuCl_2$, HBs, especially α-HB and then the like, play a very important role in stabilizing the $CuCl_2(H_2O)_n$ clusters, shortening Cu−O distance and leading to the dissociation of chloride atoms from the central ion. The formation of α-HB, β-HB, and γ-HB can enhance the hydration of the central copper atom and the charge separation between Cu and Cl atom. Especially, for $CuCl_2(H_2O)_n$ clusters ($n = 3-7$), the formation of α-HB obviously enhances the hydration of four-fold CIP conformers. Generally, the charge on the Cu atom increases as the hydrated cluster size extends, which strengthens the coordination of waters and HBs in the solvation shell. Meanwhile, the increase of electron density on the Cl atom with the dissociation of Cl anion enhances the IHBs between Cl and water molecules. Therefore, for $n = 8-10$, SSIP is iso-energetic or more stable than its CIP conformers. Our calculations present such a trend that the four-fold CIP conformer is more favorable for $CuCl_2(H_2O)_n$ clusters ($n \leq 7$) in the gas phase and four-fold SSIP/s conformer for $n = 8-10$. However, in the aqueous phase, the five-fold SSIP/s conformer is more stable than its other conformers for $n = 8$ and 9 and the four-fold CIP conformer for the smaller $CuCl_2(H_2O)_n$ clusters ($n = 2-6$). NBO charge population analyses show that there is CT between the copper atom and ligands (Cl and H_2O), as shown in Figure 1,

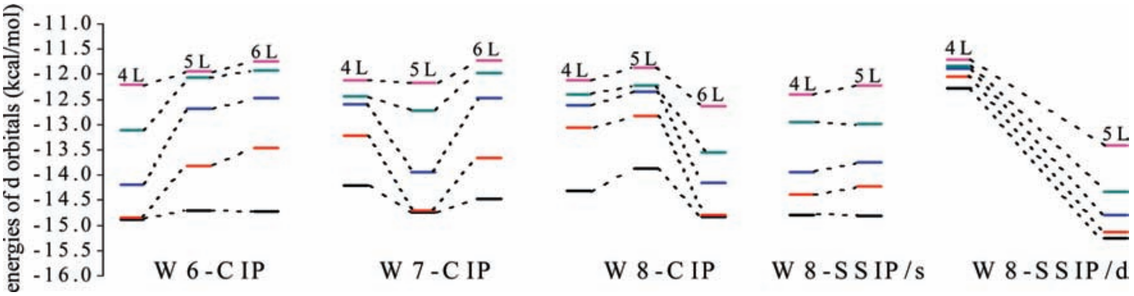

Figure 3. Energy level distributions of d orbitals of Cu^{2+} in $CuCl_2(H_2O)_n$ clusters for $n = 6-8$. $CuCl_2(H_2O)_8$, the orbital splitting of CIP, SSIP/s, and SSIP/d conformers are all shown.

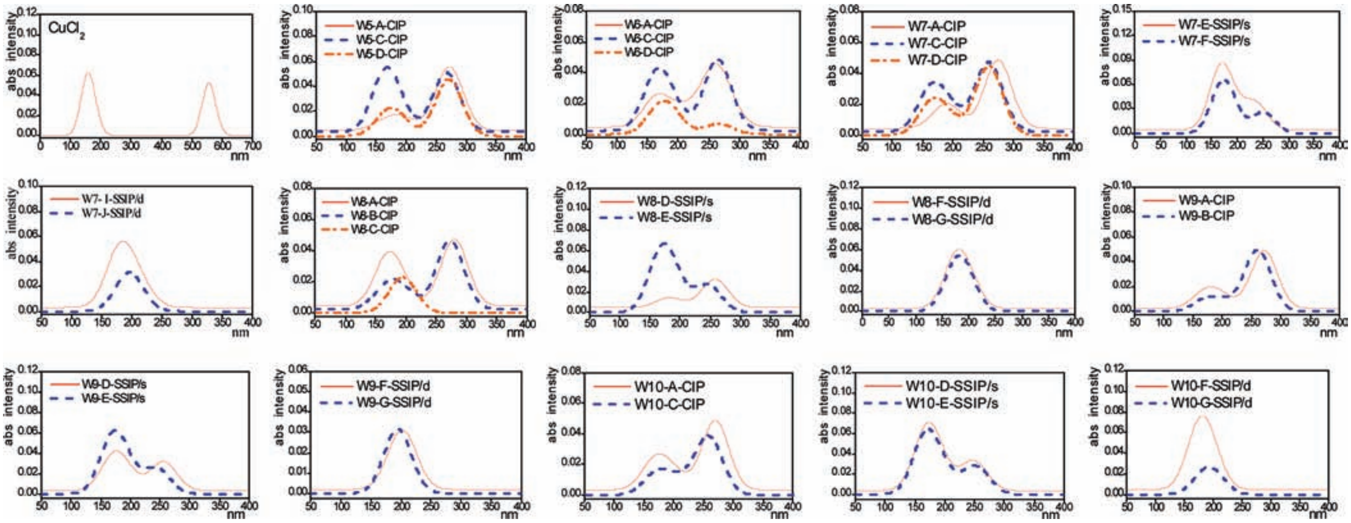

Figure 4. Calculated spectra of $CuCl_2$ molecule and $CuCl_2(H_2O)_n$ clusters for $n = 5-10$ using LRC-TDDFT/aVDZ method (298 K and 1 atm).

TABLE 3: Excited Energies (eV) and Oscillatory Strengths of $CuCl_2$ Molecule and Some Typical $CuCl_2(H_2O)_n$ Clusters for $n = 5-10$ Using LRC-TDDFT/aVDZ Method (298 K and 1 atm)

geometries		CN	excited energies (eV)[a]
$CuCl_2$[b]		2	~2.11−2.36, ~5.58
$CuCl_2$	CIP	2	$2.23_{0.16}$, $6.90_{0.02}$, $7.83_{0.10}$, $7.96_{0.07}$
$[Cu]^{2+}_{aq}$[c]	unknown	unknown	>5.51
$[CuCl]^{+}_{aq}$[c]	unknown	unknown	~4.96
$[CuCl_2]^{0}_{aq}$[c]	unknown	unknown	~4.51
W5-A	CIP	4	$4.45_{0.04}$, $4.51_{0.06}$, $4.67_{0.06}$, $6.35_{0.03}$, $7.53_{0.02}$
W5-C	CIP	5	$4.50_{0.01}$, $4.65_{0.13}$, $6.47_{0.03}$, $7.34_{0.01}$, $7.50_{0.13}$
W5-D	CIP	6	$4.56_{0.12}$, $4.68_{0.02}$, $6.55_{0.02}$, $7.26_{0.02}$, $7.33_{0.03}$
W6-A	CIP	4	$4.41_{0.03}$, $4.80_{0.10}$, $5.87_{0.03}$, $7.35_{0.03}$, $7.56_{0.03}$
W6-C	CIP	5	$4.67_{0.14}$, $6.41_{0.02}$, $6.45_{0.01}$, $7.39_{0.03}$, $7.42_{0.01}$, $7.59_{0.06}$
W6-D	CIP	6	$4.64_{0.02}$, $6.62_{0.04}$, $7.43_{0.02}$, $7.45_{0.01}$
W7-A	CIP	4	$4.51_{0.13}$, $6.37_{0.03}$, $6.77_{0.02}$
W7-C	CIP	5	$4.67_{0.01}$, $4.75_{0.10}$, $4.91_{0.03}$, $6.21_{0.01}$, $6.37_{0.03}$, $7.48_{0.02}$, $7.61_{0.04}$
W7-D	CIP	6	$4.65_{0.01}$, $4.78_{0.12}$, $4.86_{0.01}$, $6.25_{0.01}$, $6.48_{0.01}$, $7.50_{0.06}$
W8-A	CIP	4	$4.43_{0.13}$, $6.34_{0.02}$, $6.73_{0.01}$, $7.24_{0.03}$, $7.26_{0.01}$, $7.37_{0.04}$
W8-B	CIP	5	$4.54_{0.13}$, $6.23_{0.02}$, $6.87_{0.01}$, $6.99_{0.01}$, $7.44_{0.01}$, $7.47_{0.02}$
W8-C	CIP	6	$6.35_{0.03}$, $6.37_{0.03}$
W8-D	SSIP/s	4	$4.81_{0.08}$, $6.74_{0.01}$, $6.88_{0.02}$
W8-E	SSIP/s	5	$5.02_{0.08}$, $6.17_{0.01}$, $6.33_{0.01}$, $6.61_{0.02}$, $6.96_{0.01}$, $7.26_{0.05}$, $7.32_{0.06}$, $7.33_{0.05}$
W8-F	SSIP/d	4	$6.10_{0.04}$, $6.33_{0.03}$, $6.56_{0.02}$, $7.21_{0.11}$
W8-G	SSIP/d	5	$6.19_{0.02}$, $6.32_{0.05}$, $6.61_{0.02}$, $6.62_{0.02}$, $7.25_{0.09}$
W9-A	CIP	4	$4.55_{0.06}$, $4.58_{0.08}$, $6.25_{0.03}$, $7.15_{0.03}$, $7.46_{0.01}$
W9-B	CIP	5	$4.68_{0.01}$, $4.75_{0.13}$, $4.87_{0.01}$, $5.81_{0.02}$, $6.74_{0.01}$, $7.18_{0.01}$, $7.30_{0.01}$
W9-D	SSIP/s	4	$4.85_{0.08}$, $6.20_{0.02}$, $6.76_{0.01}$, $6.93_{0.02}$, $7.21_{0.08}$
W9-E	SSIP/s	5	$5.07_{0.07}$, $6.14_{0.01}$, $6.28_{0.01}$, $6.57_{0.02}$, $6.91_{0.01}$, $7.24_{0.06}$, $7.30_{0.09}$
W9-F	SSIP/d	4	$5.86_{0.02}$, $5.93_{0.01}$, $6.18_{0.03}$, $6.48_{0.02}$
W9-G	SSIP/d	5	$6.20_{0.02}$, $6.23_{0.02}$, $6.37_{0.04}$, $6.62_{0.02}$
W10-A	CIP	4	$4.59_{0.14}$, $6.01_{0.02}$, $6.37_{0.01}$, $6.97_{0.01}$, $7.36_{0.01}$, $7.47_{0.01}$, $7.48_{0.02}$
W10-C	CIP	5	$4.65_{0.03}$, $4.83_{0.09}$, $5.47_{0.07}$, $5.87_{0.01}$, $6.72_{0.02}$, $7.26_{0.02}$, $7.55_{0.02}$
W10-D	SSIP/s	4	$4.99_{0.09}$, $6.21_{0.02}$, $6.77_{0.01}$, $7.05_{0.02}$, $7.22_{0.09}$, $7.29_{0.04}$
W10-E	SSIP/s	5	$4.90_{0.08}$, $5.89_{0.02}$, $6.58_{0.03}$, $7.32_{0.10}$, $7.34_{0.07}$
W10-F	SSIP/d	4	$6.19_{0.02}$, $6.43_{0.01}$, $6.44_{0.04}$, $7.10_{0.09}$, $7.14_{0.05}$
W10-G	SSIP/d	5	$6.12_{0.01}$, $6.40_{0.04}$, $6.65_{0.02}$, $6.95_{0.01}$

[a] Oscillatory strength is presented as a suffix. [b] The peaks were observed by DeKock and Gruen in experiment at 1076 K.[59] [c] The absorption spectra were dissolved by Brugger et al. in trace $CuCl_2$ + LiCl (0−18 mol/kg) aqueous solution.[10]

and the charge separation between Cu and Cl for SSIP conformers is more apparent, which enhances the strength of IHBs, favoring the dissociation of chloride atom as *n* increases to 8.

3.2. Electronic Spectra of $CuCl_2(H_2O)_n$ Cluster. DeKock and Gruen's experimental results[59] showed that the electronic spectra of $CuCl_2$ molecule in the gas phase (1076 K) have two strong absorption peaks around 222 and 526−588 nm (~5.58 and ~2.11−2.36 eV). Our calculated electronic spectra of $CuCl_2$ by LRC-TDDFT/aVDZ method (Figure 4 and Table 3) agree well with these experimental spectra. The calculated absorption peak at ~180 nm (~6.90 eV) can be attributed to d−d transition of Cu^{2+}, while that at ~557 nm (~2.23 eV) is due to CT from the occupied p orbital of Cl atom to the d orbital

TABLE 4: OH Stretching Vibration Frequencies of Water Clusters for $n = 4-10$ Using B3LYP/aVDZ Method[a]

n	OH stretching frequencies of $(H_2O)_n$ clusters (cm^{-1})
4	$3322_{0}, 3422_{1521}, 3422_{1522}, 3461_{22}, 3863_{85}, 3864_{94}, 3863_{94}, 3865_{0}$
5	$3271_{18}, 3362_{2331}, 3370_{2193}, 3419_{66}, 3426_{66}, 3863_{67}, 3865_{74}, 3867_{61}, 3868_{55}, 3870_{68}$
6	$3273_{5}, 3341_{2718}, 3364_{2552}, 3407_{457}, 3423_{0}, 3434_{166}, 3864_{68}, 3864_{75}, 3867_{33}, 3868_{73}, 3877_{135}, 3877_{1}$
7	$3111_{781}, 3235_{1432}, 3381_{653}, 3455_{553}, 3562_{290}, 3571_{417}, 3656_{489}, 3681_{191}, 3743_{316}, 3818_{105}, 3863_{44}, 3864_{55}, 3866_{119}, 3868_{67}$
8	$3164_{3}, 3190_{21}, 3218_{1725}, 3223_{1726}, 3581_{473}, 3585_{154}, 3586_{148}, 3596_{1}, 3617_{2}, 3646_{678}, 3648_{680}, 3664_{1095}, 3862_{84}, 3862_{79}, 3863_{40}, 3863_{48}$
9	$3155_{15}, 3179_{64}, 3210_{1779}, 3211_{1919}, 3286_{1086}, 3568_{321}, 3578_{284}, 3583_{243}, 3592_{68}, 3609_{17}, 3638_{661}, 3643_{697}, 3660_{1147}, 3759_{62}, 3862_{73}, 3862_{51}, 3864_{64}, 3868_{61}$
10	$2857_{1392}, 3177_{1208}, 3299_{664}, 3386_{605}, 3405_{574}, 3465_{222}, 3469_{829}, 3521_{662}, 3578_{577}, 3615_{345}, 3627_{380}, 3683_{189}, 3710_{480}, 3731_{507}, 3753_{278}, 3855_{55}, 3859_{64}, 3861_{86}, 3863_{58}, 3864_{90}$

[a] IR Intensities given in subscripts are in 10 km/mol.

TABLE 5: OH Stretching Vibration Frequencies of $CuCl_2(H_2O)_n$ Clusters for $n = 4-10$ Using B3LYP/aVDZ Method[a]

geometries	n	OH stretching frequencies of $CuCl_2(H_2O)_n$ clusters (cm^{-1})
CIP	4	$3201_{1730}, 3204_{216}, 3570_{923}, 3571_{70}, 3793_{48}, 3794_{162}, 3854_{127}, 3854_{82}$
CIP	5	$3238_{986}, 3317_{477}, 3366_{1250}, 3594_{490}, 3604_{578}, 3627_{279}, 3781_{112}, 3855_{134}, 3856_{63}, 3858_{125}$
CIP	6	$3325_{933}, 3341_{38}, 3368_{5}, 3378_{2542}, 3610_{78}, 3611_{1545}, 3618_{156}, 3622_{19}, 3857_{6}, 3857_{343}, 3857_{20}, 3858_{63}$
CIP	7	$2994_{839}, 3062_{947}, 3267_{1116}, 3299_{791}, 3534_{367}, 3598_{222}, 3625_{162}, 3648_{572}, 3689_{431}, 3739_{105}, 3759_{154}, 3778_{84}, 3854_{88}, 3854_{59}$
SSIP/S	8	$2907_{1210}, 3020_{829}, 3193_{250}, 3244_{1750}, 3525_{352}, 3534_{482}, 3600_{176}, 3612_{300}, 3669_{512}, 3739_{127}, 3746_{218}, 3765_{340}, 3785_{80}, 3811_{83}, 3848_{70}, 3856_{72}$
SSIP/d	8	$2821_{121}, 2860_{950}, 2984_{2510}, 3113_{1014}, 3219_{861}, 3288_{633}, 3413_{83}, 3430_{309}, 3501_{1104}, 3511_{124}, 3522_{1518}, 3532_{437}, 3560_{761}, 3858_{99}, 3859_{89}, 3868_{77}$
SSIP/S	9	$3072_{632}, 3080_{319}, 3110_{514}, 3159_{2605}, 3282_{1677}, 3358_{519}, 3387_{158}, 3420_{586}, 3527_{1033}, 3532_{1200}, 3541_{247}, 3579_{420}, 3740_{46}, 3749_{281}, 3841_{77}, 3856_{90}, 3859_{79}, 3859_{77}$
SSIP/d	9	$2483_{559}, 2596_{57}, 2679_{4334}, 3123_{535}, 3194_{1541}, 3343_{471}, 3358_{1014}, 3378_{609}, 3407_{646}, 3447_{782}, 3536_{675}, 3558_{266}, 3572_{598}, 3609_{846}, 3798_{87}, 3847_{99}, 3853_{103}, 3855_{72}$
SSIP/S	10	$2937_{911}, 3056_{281}, 3077_{146}, 3109_{3334}, 3159_{1143}, 3369_{88}, 3395_{196}, 3406_{799}, 3460_{651}, 3499_{1119}, 3506_{1170}, 3570_{233}, 3577_{668}, 3652_{376}, 3728_{165}, 3736_{344}, 3834_{70}, 3851_{87}, 3858_{82}, 3866_{79}$
SSIP/d	10	$2774_{932}, 2783_{1126}, 2880_{873}, 2968_{1483}, 3091_{185}, 3277_{594}, 3297_{1286}, 3300_{691}, 3324_{232}, 3398_{354}, 3418_{780}, 3434_{1047}, 3442_{376}, 3459_{207}, 3561_{117}, 3608_{169}, 3846_{109}, 3852_{88}, 3863_{83}, 3863_{79}$

[a] IR intensities given as subscripts are in 10 km/mol.

of the copper atom. Therefore, calculations of electronic absorption spectra for hydrated $CuCl_2(H_2O)_n$ ($n = 5-10$) clusters were also performed at the LRC-TDDFT/aVDZ level. Figure 4 presents the calculated electronic absorption spectra of typical CIP and SSIP $CuCl_2(H_2O)_n$ conformers for $n = 5-10$ in the gas phase, which are compared with the UV−vis−NIR spectrum of trace Cu(II) chloride in LiCl aqueous solution from dilute to 18 mol/kg[10] and the spectrum of the $CuCl^+$ complex in aqueous solution.[11]

The calculated spectra of all four- and five-fold CIP $CuCl_2(H_2O)_n$ clusters for $n = 5-10$ have two absorption bands at ~180 and ~270 nm, as shown in Figure 4, which can be attributed to d−d transition of Cu^{2+} and CT between the central copper atom and ligands (Cl and H_2O), respectively. These two bands are also found in the six-fold CIP conformer for all $CuCl_2(H_2O)_n$ ($n = 5-7$) clusters; however, the peak at ~270 nm disappears for the six-fold CIP $CuCl_2(H_2O)_8$ conformer. With the increasing water molecules, the absorption of the d−d transition is red-shifted, and that of CT between the central copper atom and ligands is blue-shifted. For SSIP/s conformers, there are also two absorption bands (around 180 and 250 nm) that can be also attributed to d−d transition and CT in $CuCl_2(H_2O)_n$ clusters, respectively. However, the CT band is blue-shifted in comparison to that of CIP conformers. The same as CIP conformers, d−d transition and CT bands for the SSIP/s cluster are red-shifted and blue-shifted as the number of attached water molecules increases, respectively. In contrast, there is only one obvious absorption peak around ~180 nm for those SSIP/d conformers, which can be mainly attributed to d−d transition of Cu^{2+}.

Brugger et al.[10] have measured the spectra of trace $CuCl_2$ in LiCl solutions and dissolved the measured spectra assuming that hydrated $[CuCl_n]^{2-n}$ ($n = 0-4$) species exist in it. For the assumed $[CuCl_2]^0_{aq}$ species, they obtained a dissolved absorption peak at 275 nm, which is very likely to be CIP conformers with four- or five-coordination number according to our theoretical calculation. The six-fold CIP conformers for the $CuCl_2(H_2O)_n$ cluster seem impossible since their hydration energies ΔE are far smaller than that of four- or five-fold CIP structures. In addition, the $[CuCl_2]^0_{aq}$ species may not be the SSIP/d conformer of the $CuCl_2(H_2O)_n$ cluster for there is only one peak (around 180 nm), and the SSIP/s conformer is possible as long as the water molecule is sufficient. However, the absorption peaks around 250 and 180 nm for SSIP/s and SSIP/d conformers, respectively, probably correspond to $[CuCl]^+_{aq}$ and $[Cu]^{2+}_{aq}$ species resolved from experimental spectra.[10,11]

3.3. Frequency Analysis−IR Spectra. The OH stretching vibration frequency is widely used to identify diverse cluster structures, and thus all of the OH stretching vibration frequencies of water clusters and the most stable CIP and SSIP $CuCl_2(H_2O)_n$ clusters for $n = 4-10$ in the gas phase were calculated at the B3LYP/aVDZ level and are presented in Table 4 and Table 5, respectively. In cluster scale, water molecules can be classified as "D", "A", "DA", "AA", "DAA", "DD", "DDA", and "DDAA" types, where D and A indicate H-donor and H-acceptor, respectively. For comparing IR spectra of $CuCl_2(H_2O)_n$ clusters, those of water clusters for $n = 4-10$ were also calculated at the B3LYP/aVDZ level, as shown in Table 4.

The spectra of CIP $CuCl_2(H_2O)_n$ conformers for $n = 4-7$ have two obvious bands (~3750 and ~3850 cm^{-1}) in the high-frequency region. However, the frequencies of these vibrations (~3750 and ~3850 cm^{-1}) are substantially red-shifted in comparison to those of free water molecule (~3800 and ~3900 cm^{-1}) because of partial CT between the central copper atom and the surrounding ligands (Cl and H_2O). For CIP $CuCl_2(H_2O)_n$ conformers, the peaks at ~3600 and ~3850 cm^{-1} can be attributed to the free OH stretching vibration frequencies of solvation shell water molecules that only form A-type HB, while the bands at ~3200 and ~3790 cm^{-1} are the OH and free OH stretching vibration frequencies of D-type water molecules. The

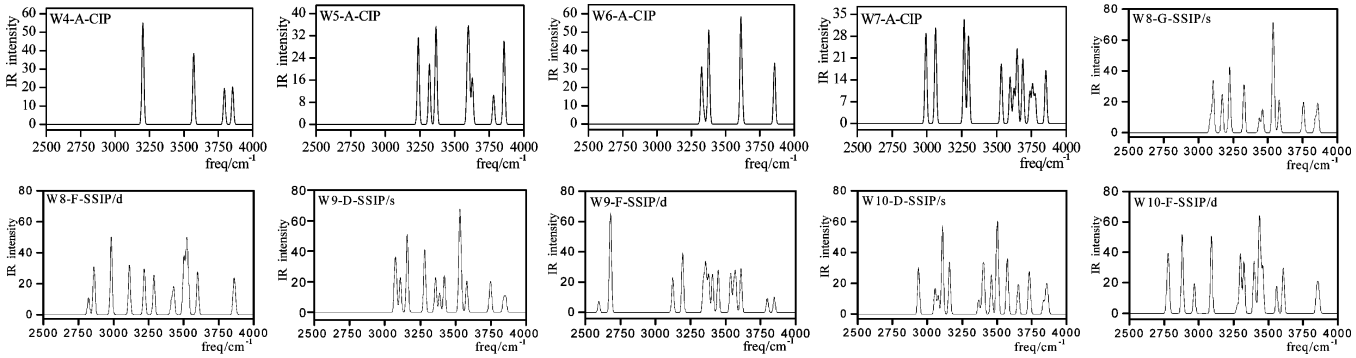

Figure 5. IR spectra of $CuCl_2(H_2O)_n$ clusters for $n = 4-10$ using B3LYP/aVDZ method (298 K and 1 atm).

bands at $\sim$3330 and $\sim$3370 cm^{-1} can be attributed to the ν_{sym} and ν_{asym} of DD water molecules in the solvation shell. The calculated OH and free OH stretching vibration frequencies of DA water molecules in W7-A are $\sim$3630 and $\sim$3760 cm^{-1}, respectively. There are two obvious bands around 3000 cm^{-1} that are attributed to OH stretching vibration frequencies of D- and AD-type water molecules in W7-A, which is different from those for $n = 4-6$, probably due to the formation of a HB network. Those free OH stretching vibration frequencies of CIP $CuCl_2(H_2O)_n$ complexes for $n = 4-7$ are red-shifted as the hydrated cluster expands because the magnitude of CT from Cu to water molecule decreases. Similar trends have been also observed in the spectra of $Ca^{2+}(H_2O)_n$.[60]

Similar to CIP $CuCl_2(H_2O)_n$ clusters, for the lowest-energy structures of the SSIP conformer ($n = 8-10$), there is an obvious absorption band in the high-frequency region (around $\sim$3850 cm^{-1}) besides other peaks, and OH stretching vibration frequencies of the SSIP clusters are also red-shifted as the number of attached water molecules increases. However, for SSIP configurations, stretching vibration frequencies of OH interacting with the dissociated chloride atoms have a lower range of $\sim$2700$-$3100 cm^{-1}, and especially for SSIP/d conformers, an obvious absorption peak can be found in the range of $\sim$2700$-$2800 cm^{-1}, which was not observed in copper$-$water complexes.[22] In addition, compared to those of water clusters, OH stretching vibration frequencies of a D-type water molecule in $CuCl_2(H_2O)_n$ complexes (CIP, SSIP conformers) are obviously red-shifted due to CT between the central copper atom and the surrounding ligands, which leads to the enhancement of HBs in those hydrated clusters.

4. Conclusions

In the present paper, the hydrates of copper dichloride have been investigated using the B3LYP/aVDZ method. Our calculations show that the coordination number of central Cu(II) atom varies with different hydration states. Four-fold CIP conformers are the most stable structure in the gas phase ($n \leq 7$), while in the aqueous phase, the five-fold SSIP/s conformer is slightly more stable than CIP conformer of $CuCl_2(H_2O)_n$ for $n \leq 7$ with an exception for $n = 10$. α-HBs play an important role in stabilizing $CuCl_2(H_2O)_n$ complexes, which is consistent with the reported articles.[14−17] From our estimation, seven water molecules may be enough for the solvation of $CuCl_2$, and more water molecules involved in the inner solvation shell will lead to the dissocitation of Cl^-. NBO charge population analyses of $CuCl_2(H_2O)_n$ clusters suggest that the charge separation between the central copper atom and chloride atoms is strengthened by α-HBs and β-HBs among hydration shells. Due to the dissociation of two Cl^-, the SSIP/d conformer of $CuCl_2(H_2O)_n$ clusters for $n = 7-10$ has only one absorption peak (around 180 nm) which can be attributed to d$-$d transition of Cu^{2+}. Our calculated electronic absorption spectra around 270 nm (due to CT) of CIP conformers using LRC-TDDFT/aVDZ method are coincident with the spectrum[10] for $[CuCl_2]^0_{aq}$ species dissolved from the experimental spectra in trace $CuCl_2$ + LiCl (0$-$18 mol/kg) aqueous solution, while the CT band (around 250 nm) of SSIP/s and d$-$d transition band (around 180 nm) of SSIP/d conformers probably correspond to the absorption peaks for $[CuCl]^+_{aq}$ and $[Cu]^{2+}_{aq}$ species, respectively. OH stretching vibration frequencies of CIP and SSIP clusters are red-shifted as the cluster size extends because the HBs are strengthened in those clusters as the hydration proceeds. The OH stretching vibration bands of SSIP conformers are red-shifted in comparison to those of its CIP isomer, for more CT in SSIP conformers. In addition, OH stretching vibration frequencies of the D-type water molecule in $CuCl_2(H_2O)_n$ complexes are apparently red-shifted for CT between Cu and ligands (Cl and H_2O) compared to those of the corresponding water clusters $(H_2O)_n$. It can be seen from the above calculations and discussions that even the structures of $CuCl_2(H_2O)_n$ species in the aqueous phase are already quite complicated, and a complete insight into the structures of copper dichloride complexes in aqueous solution cannot be gained until a series of theoretical investigations on other hydrated cupric chloride complexes in aqueous phase, such as $[Cu]^{2+}_{aq}$, $[CuCl]^+_{aq}$, $[CuCl_3]^-_{aq}$, and $[CuCl_4]^{2-}_{aq}$ species, have been carried out.

Acknowledgment. This work was financially supported by the National Natural Science Foundation of China under Contract Number 20773036. H.B.Y. acknowledges the support of "985" Foundation of the Ministry of Education of China. We thank the reviewers for suggestions, which help us improve this work.

Supporting Information Available: More optimized local minimum energy structures and energy parameters of $CuCl_2(H_2O)_n$ for $n = 1-10$ at the B3LYP/aVDZ level and more electronic absorption spectra at the LRC-TDDFT/aVDZ level. This material is available free of charge via the Internet at http://pubs.acs.org.

References and Notes

(1) McDonald, R. G.; Muir, D. M. *Hydrometallurgy* **2007**, *86*, 206–220.

(2) Senanayake, G. *Miner. Eng.* **2007**, *20*, 1075–1088.

(3) Park, K.-H.; Mohapatra, D.; Kim, H.-I.; Guo, X. *Sep. Purif. Technol.* **2007**, *56*, 303–310.

(4) Vilcu, R.; Madrinan, E.C. D.; Irinei, F. *Rev. Roum. Chim.* **1976**, *21*, 333–341.

(5) Filippov, V. K.; Charykov, N. A.; Fedorov, Yu. A. *Zh. Neorg. Khim.* **1986**, *31*, 1861–1866.

(6) Vlasenko, K. K.; Karapet'yants, M. Kh. *Zh. Fiz. Khim.* **1971**, *45*, 2460–2463.

(7) Bjerrum, J. *K. Dan. Vidensk. Selsk. Mat-Fys. Medd.* **1946**, *22*, 1–43.

(8) Khan, M. A.; Schwing-weill, M. J. *Inorg. Chem.* **1976**, *15*, 2202–2205.

(9) Bjerrum, J. *Acta Chem. Scand.* **1987**, *A41*, 328–334.

(10) Brugger, J.; Mcphail, D. C.; Black, J.; Spiccia, L. *Geochim. Cosmochim. Acta* **2001**, *65*, 2691–2708.

(11) Libus, Z. *Inorg. Chem.* **1973**, *12*, 2972–2977.

(12) Petersen, C. P.; Gordon, M. S. *J. Phys. Chem. A* **1999**, *103*, 4162–4166.

(13) Yang, Y.; Meng, Sh.; Xu, L. F.; Wang, E. G. *Phys. Rev.* **2005**, *72*, 012602-1–012602-4.

(14) Olleta, A. C.; Lee, H. M.; Kim, K. S. *J. Chem. Phys.* **2006**, *124*, 024321-1–024321-12.

(15) Singh, N. J.; Yi, H.-B.; Min, S. K.; Park, M.; Kim, K. S. *J. Phys. Chem. B* **2007**, *110*, 3808–3815.

(16) Olleta, A. C.; Lee, H. M.; Kim, K. S. *J. Chem. Phys.* **2007**, *126*, 144311-1–144311-11.

(17) Petit, L.; Vuilleumier, R.; Maldivi, P.; Adamo, C. *J. Chem. Theory Comput.* **2008**, *4*, 1040–1048.

(18) Berces, A.; Nukada, T.; Margl, P.; Ziegler, T. *J. Phys. Chem. A* **1999**, *103*, 9693–9701.

(19) Schwenk, C. F.; Rode, B. M. *J. Am. Chem. Soc.* **2004**, *126*, 12786–12787.

(20) Duncombe, B. J.; Duale, K.; Smith, A. B.; Stace, A. J. *J. Phys. Chem. A* **2007**, *111*, 5158–5165.

(21) Sukart, K.; Parasuk, V. *Chem. Phys. Lett.* **2007**, *447*, 58–64.

(22) O'Brien, J. T.; Williams, E. R. *J. Phys. Chem. A* **2008**, *112*, 5893–5901.

(23) Bryantsev, V. S.; Diallo, M. S.; van Duin, A. C. T.; Goddard, W. A., III. *J. Phys. Chem. A* **2008**, *112*, 9104–9112.

(24) Garcia, J.; Benfatto, M.; Natoli, C. R.; Bianconi, A.; Fontaine, A.; Tolentino, H. *Chem. Phys.* **1989**, *132*, 295–307.

(25) Beagley, B.; Eriksson, A.; Lindgren, J.; Persson, I.; Pettersson, L. G. M.; Sandström, M.; Wahlgren, U.; White, E. W. *J. Phys.: Condens. Matter* **1989**, *1*, 2395–2408.

(26) Pasquarello, A.; Petri, I.; Salmon, P. S.; Parisel, O.; Car, R.; Toth, E.; Powell, D. H.; Fischer, H. E.; Helm, L.; Merbach, A. E. *Science* **2001**, *291*, 856–859.

(27) Benfatto, M.; D'Angelo, P.; Della Longa, S.; Pavel, N. V. *Phys. Rev. B* **2002**, *65*, 174205-1–174205-5.

(28) Burda, J. V.; Pavelka, M.; Šimánek, M. *J. Mol. Struct. (THEOCHEM)* **2004**, *683*, 183–193.

(29) Lee, H. M.; Min, S. K.; Lee, E. C.; Min, J. H.; Odde, S.; Kim, K. S. *J. Chem. Phys.* **2005**, *122*, 064314-1–064314-10.

(30) Pranowo, H. D.; Bambang Setiaji, A. H.; Rode, B. M. *J. Phys. Chem. A* **1999**, *103*, 11115–11120.

(31) Shang, L. B.; Bi, X. Wu.; Hu, R. Zh.; Fan, W. L. *Chin. Sci. Bull.* **2007**, *52*, 395–400.

(32) Iikura, H.; Tsuneda, T.; Yanai, T.; Hirao, K. *J. Chem. Phys.* **2001**, *115*, 3540–3544.

(33) Tawada, Y.; Tsuneda, T.; Yanagisawa, S.; Yanai, T.; Hirao, K. *J. Chem. Phys.* **2004**, *120*, 8425–8433.

(34) Rohrdanz, M. A.; Martins, K. M.; Herberta, J. M. *J. Chem. Phys.* **2009**, *130*, 054112-1–054112-8.

(35) (a) Hammer, N. I.; Shin, J. W.; Headrick, J. M.; Diken, E. G.; Roscioli, J. R.; Weddle, G. H.; Johnson, M. A. *Science* **2004**, *306*, 675–679. (b) Barckholtz, T. A.; Miller, T. A. *J. Phys. Chem. A* **1999**, *103*, 2321–2336. (c) Pribble, R. N.; Zwier, T. S. *Science* **1994**, *265*, 75–79.

(36) (a) Brutschy, B. *Chem. Rev.* **2000**, *100*, 3891–3920. (b) Kim, K. S.; Tarakeshwar, P.; Lee, J. Y. *Chem. Rev.* **2000**, *100*, 4145–4186. (c) Bieske, E. J.; Dopfer, O. *Chem. Rev.* **2000**, *100*, 3963–3998.

(37) Buck, U.; Ettischer, I.; Melzer, M.; Buch, V.; Sadlej, J. *Phys. Rev. Lett.* **1998**, *80*, 2578–2581.

(38) (a) Lee, H. M.; Suh, S. B.; Lee, J. Y.; Tarakeshwar, P.; Kim, K. S. *J. Chem. Phys.* **2000**, *112*, 9759–9772. (b) Lee, H. M.; Suh, S. B.; Kim, K. S. *J. Chem. Phys.* **2003**, *119*, 7685–7692. (c) Odde, S.; Mhin, B. J.; Lee, S.; Lee, H. M.; Kim, K. S. *J. Chem. Phys.* **2004**, *120*, 9524–9535.

(39) Bertrn, J.; Rodrguez-Santiago, L.; Sodupe, M. *J. Phys. Chem. B* **1999**, *103*, 2310–2317.

(40) Rimola, A.; Rodrguez-Santiago, L.; Ugliengo, P.; Sodupe, M. *J. Phys. Chem. B* **2007**, *111*, 5740–5747.

(41) Dunning, T. H., Jr. *J. Chem. Phys.* **1989**, *90*, 1007–1023.

(42) Dolg, M.; Wedig, U.; Stoll, H.; Preu, H. *J. Chem. Phys.* **1987**, *86*, 866–872.

(43) Boys, S. F.; Bernardi, F. *Mol. Phys.* **1970**, *19*, 553–566.

(44) Dombroski, J.; Head-Gordon, M.; Gilbert, A. *Q-Chem*, revision 3.2; Pittsburgh, PA, 2009.

(45) Glendening, E. D.; Reed, A. E. ; Carpenter, J. E.; Weinhold, F. *NBO*, version 3.1.

(46) (a) Foster, J. P.; Weinhold, F. *J. Am. Chem. Soc.* **1980**, *102*, 7211–7218. (b) Reed, A. E.; Weinhold, F. *J. Chem. Phys.* **1983**, *78*, 4066–4073. (c) Reed, A. E.; Curtiss, L. A; Weinhold, F. *Chem. Rev.* **1988**, *88*, 899–926.

(47) Goodman, L; Sauers, R. *J. Chem. Theory Comput.* **2005**, *1*, 1185–1192.

(48) Bryantsev, V. S.; Diallo, M. S.; Goddard, W. A., III. *J. Phys. Chem. B* **2008**, *112*, 9709–9719.

(49) Wander, M. C. F.; Clark, A. E. *Inorg. Chem.* **2008**, *47*, 8233–8241.

(50) Mennucci, B.; Tomasi, J. *J. Chem. Phys.* **1997**, *107*, 3032–3041.

(51) Mennucci, B.; Cances, E.; Tomasi, J. *J. Phys. Chem. B* **1997**, *101*, 10506–10517.

(52) Frisch, M. J.; Trucks, G. W.; Schlegel, H. B.; Scuseria, G. E.; Robb, M. A.; Cheeseman, J. R.; Zakrzewski, V. G.; Montgomery, J. A., Jr.; Stratmann, R. E.; Burant, J. C.; Dapprich, S.; Millam, J. M.; Daniels, A. D.; Kudin, K. N.; Strain, M. C.; Farkas, O.; Tomasi, J.; Barone, V.; Cossi, M.; Cammi, R.; Mennucci, B.; Pomelli, C.; Adamo, C.; Clifford, S.; Ochterski, J.; Petersson, G. A.; Ayala, P. Y.; Cui, Q.; Morokuma, K.; Salvador, P.; Dannenberg, J. J.; Malick, D. K.; Rabuck, A. D.; Raghavachari, K.; Foresman, J. B.; Cioslowski, J.; Ortiz, J. V.; Baboul, A. G.; Stefanov, B. B.; Liu, G.; Liashenko, A.; Piskorz, P.; Komaromi, I.; Gomperts, R.; Martin, R. L.; Fox, D. J.; Keith, T.; Al-Laham, M. A.; Peng, C. Y; Nanayakkara, A.; Challacombe, M.; Gill, P. M. W.; Johnson, B.; Chen, W.; Wong, M. W.; Andres, J. L.; Gonzalez, C.; Head-Gordon, M.; Replogle, E. S.; Pople, J. A. *Gaussian 03*, revision E.01; Gaussian, Inc.: Pittsburgh, PA, 2003.

(53) Chase, M. W., Jr. *J. Phys. Chem. Ref. Data*, **1998**; Monograph 8, pp 1−1951.

(54) Dunn, K. M.; Morokuma, K. *J. Phys. Chem.* **1996**, *100*, 123–129.

(55) Witek, H. A.; Kohler, C.; Frauenheim, T.; Morokuma, K.; Elstner, M. *J. Phys. Chem. A* **2007**, *111*, 5712–5719.

(56) Magini, M. *J. Chem. Phys.* **1981**, *74*, 2523–2529.

(57) D'Angelo, P.; Bottari, E.; Festa, M. R. *J. Chem. Phys.* **1997**, *107*, 2807–2812.

(58) Ansell, S.; Tromp, R. H.; Neilson, G. W. *J. Phys.: Condens. Mater* **1995**, *7*, 1513–1524.

(59) DeKock, C. W.; Gruen, D. M. *J. Chem. Phys.* **1966**, *44*, 4387–4398.

(60) Bush, M. F.; Saykally, R. J.; Williams, E. R. *ChemPhysChem* **2007**, *8*, 2245–2253.

JP909092P